Structural Analysis Using Integrated Geophysical Methods for Suspected Gold Mineralization within New Peyi Area, Ushafa – Bwari, Abuja, Northcentral Nigeria.

Stephen Onuzuruike Udeh[1], Patrick N. Dikedi[2], Martin Ogharandukun[3], Uko Ofe[4], Okolo Ikechukwu Thaddeaus [5], and Akinde Aderibigbe [6]

[1]Department of Pure and Applied Physics, Faculty of Natural and Applied Sciences, Veritas University. Abuja.

[2]Department of Pure and Applied Physics, Faculty of Natural and Applied Sciences, Veritas University. Abuja.

[3]Department of Pure and Applied Physics, Faculty of Natural and Applied Sciences, Veritas University. Abuja.

[4]Department of Pure and Applied Physics, Faculty of Natural and Applied Sciences, Veritas University. Abuja.

[5]National Steel Raw Materials Exploration Agency, Kaduna – Nigeria

[6]Slyvopetro International Limited, Abuja - Nigeria

Stephen O. Udeh Email: stephenudeh2010@gmail.com †M.Sc. Researcher (Address: National Steel Raw Materials Exploration Agency, No. 18 Rabba Road, Malali – Kaduna, Nigeria)

Key Points: Structural Analysis, Integrated Geophysical Methods, Suspected Gold Mineralization

Abstract

In the structural analysis of New Peyi integrated geophysical methods were employed to determine portions of gold mineralization. The area is bounded by latitudes 09° 13' 16.8" N and 09° 13' 33.1" N, and longitudes 007° 23' 00.2" E and 007° 23' 16.6" E. The total area coverage is 250,000 m^2. The Instruments used were GSM-19 Overhauver, GSMP-25 Potassium magnetometers and ABEM SAS 1000 Terrameter. The main faults run approximately in a North-South direction. Magnetic readings were taken along eleven profile lines, 500 meters long, (in an East-West direction), and uniformly spaced 50 meters apart. The acquired corrected magnetic data were used in developing the Total Magnetic Intensity map of the area which was subsequently filtered. The residual magnetic values range from -4643.3 nanotesla to 2310.3 nanotesla, characterizing regions with low negative amplitudes, (high wavelengths - indicating shallow causative body). The results from the Analytical Signal determine the geometry and correct position of the magnetic bodies, while the source parameter imaging (SPI) map estimated the deepness of mineralization to be less than 27 meters. The induced polarization data obtained along four profile lines arranged in an East-West direction were used to produce 2-dimensional inversion models that allowed for the identification of areas of high chargeability (above 4.5 millivolt/Volt) and/or high resistivity, possibly attributed to mineralization. The areas with low values (below 2.0 millivolt/Volt) are associated with barren soils and rocks. The induced polarization method results show a depth variation between 9.0 meters – 24.5 meters.

The Plain Language Summary

A combination of different geophysical methods was applied to study the structural control of gold mineralization within New Peyi, Bwari. The area is bounded by latitudes 09° 13' 16.8" N and 09° 13' 33.1" N, and longitudes 007° 23' 00.2" E and 007° 23' 16.6" E. The total area is 250,000 m^2. The instruments used for data collection were magnetometers (for the magnetic data) and Terrameter (for the geoelectric data).

Magnetic readings were taken along eleven profile lines, each 500 meters long, parallel to one another (in an east–west orientation), and uniformly spaced 50 meters apart. The magnetic data acquired were used to produce a combined regional/residual magnetic image of the area which was subsequently filtered to enhance interpretations. From the results obtained the estimated depth of mineralization is less than 27 meters. The induced polarization data obtained along four profile lines in the same orientation were used to produce 2-dimensional models that helped in identifying areas of high chargeability and/or high resistivity, indicative of possible mineralization. The areas with low values (below 2.0 millivolt/Volt) show barren soils and rocks. The induced polarization method results show a depth variation between 9.0 meters – 24.5 meters.

1.0 Introduction

According to Abdullahi and Alabi, (2018), Nigerian gold deposits are generally described by various earth deformation processes and structure traversed by regional northwest-southeast fault-fracture zones. Chuku, (1981), in Abdullahi and Alabi, (2018) opined that in Nigeria's basement complex migmatization and deformation of the metamorphic rocks resulted in the distribution of gold mineralization in quartz veins.

The geophysical exploration methods to be employed depend upon the geological characteristics of a given mineral deposit. In Nigeria's schist belts, economic gold occurs in three forms including alluvial, eluvial, and primary veins deposits. Mbonimpa *et al*., (2007) are of the view that primary gold normally occurs together with pyrrhotite, magnetite, and ilmenite in igneous intrusions. Ground magnetic and geoelectrical (resistivity and induced polarization) methods were carried out within the project area to delineate possible gold mineralization.

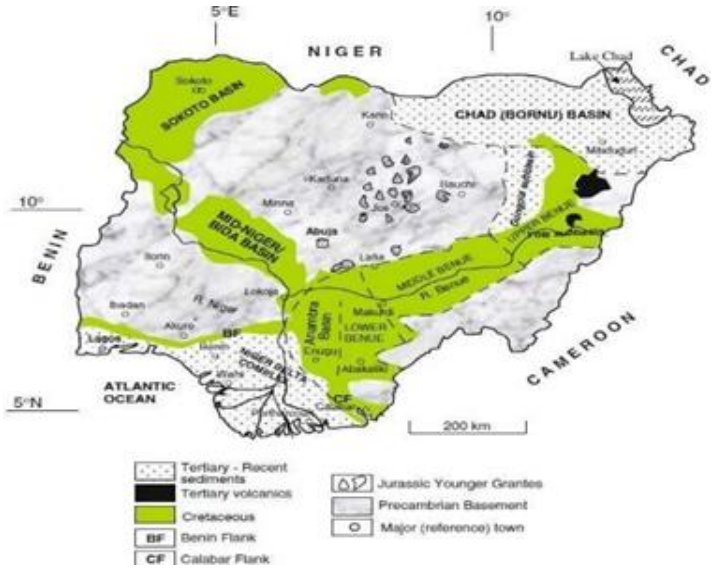

Fig. 1: Geological Map of Nigeria: Obaje, (2009).

1.1 Geological Synopsis of Abuja

Abuja and its environs lie within the crystalline basement complex terrain of North-central Nigeria. The basement complex, a part of repeatedly metamorphosed West African craton dominated about 60% of Nigeria's gneisses, schists, and a host of other metamorphosed and granitic rocks.

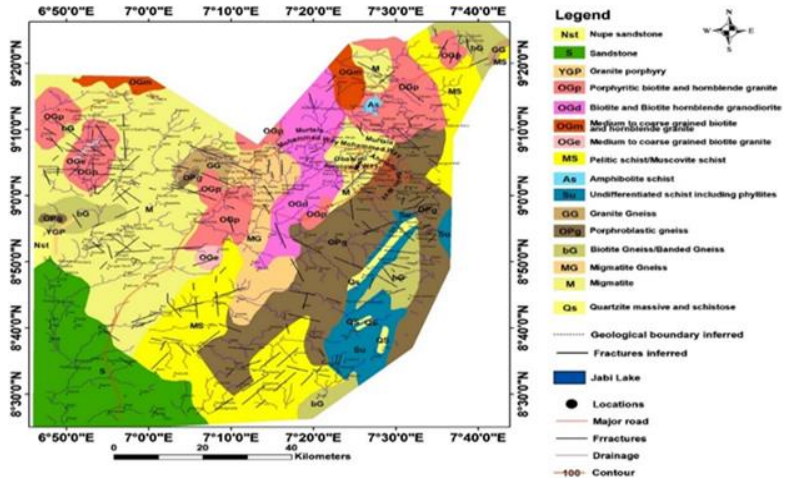

Fig. 2: Geologic Map of the Federal Capital Territory, Abuja. NGSA, (2004).

The geologic deposits found in Abuja include various types of gneisses, schists, quartzites, amphibolites and granites.

1.2 Geology of New Peyi - Ushafa

New Peyi–Ushafa lies within the northcentral schist belt of Nigeria. Its geology is composed mainly of granites, gneisses, schists and migmatites sometimes partly overlain by superficial laterite deposits, gravels, and soils. Iron-stained, dirty quartzites occasionally intruded the schists.

The dendritic drainage pattern of the streams in the area is guided by the fractures and joints in these rocks. Two main flow directions due to major structural patterns are N – S, and NW – SE.

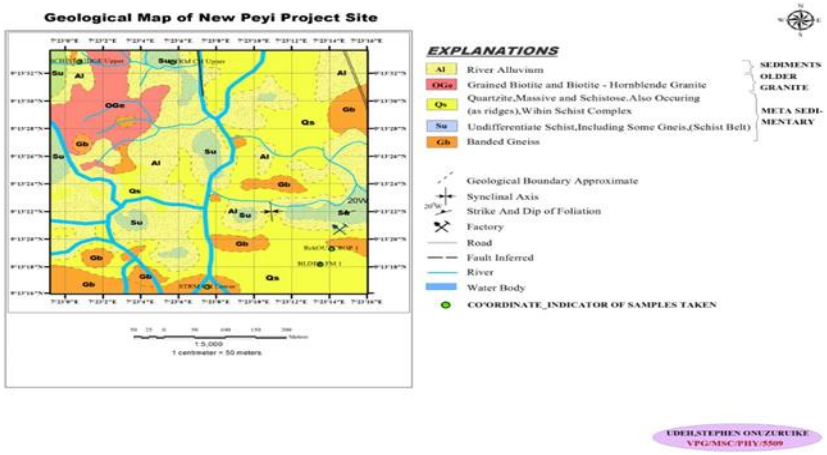

Fig. 3: Geological Map of New Peyi - Ushafa.

The New Peyi - Ushafa area is immensely enriched with mineral deposits of enormous economic importance including quartzites, river gravels, granite, and gold. The gold occurrences within the study area being controlled structurally, are mainly of primary origin.

2.0 Materials and Methods

2.1 Materials

GSM-19 Overhauver (Base Station Console) and GSMP-25 Potassium Magnetometer (Walkmag Console) and their accessories, manufactured by GEM SYSTEMS, Canada, were employed during magnetic survey measurements. The software for data processing and enhancements included GEM software for diurnal correction and Geosoft Oasis montaj.

The acquisition of geo-electrical data was carried out using ABEM SAS 1000 Terrameter. Res2Dinv software was used for the data processing.

2.2 Methods

For the correction of diurnal variations base station was set up at a position that is free from magnetic interferences. It was kept at a fixed point throughout the survey, while the walk-mag rover and console were used to traverse the established profile lines for the data acquisition.

The survey design enabled eleven (11) profile lines - each 500 m long, and trending east-west, aligned orthogonally to the strike direction of the host rock – to be covered using workmag GSMP-25 Potassium Magnetometer. The acquired data was downloaded from the instrument into a computer system. These were subsequently inputted and preserved in an Excel Spreadsheet for further action. The inbuilt GPS **(**datum - WGS84) enabled the synchronous tying of the magnetic stations to their respective coordinate locations. Visual inspections were carried out for data quality enhancement and assurance. All available sources of disturbances were also noted including communication masks, high-tension lines, and other metallic structures.

Furthermore, the results from the TMI were imperative in delineating promising anomalous areas that were subjected to additional survey using ABEM SAS 1000 Terrameter configured to simultaneously carry out apparent resistivity imaging and induced polarization (IP) using the Wenner Array method.

The IP method involves an application of external electrical energy which, when switched off abruptly, makes the voltage drop rapidly from its initial value $\mathbf{V_0}$ to a non-zero value $\mathbf{V_1}$ (stage A), and thereafter completely decays slowly (stage B), in a polarizable ground. This transient behaviour is known as the time-domain IP effect. It is this transient decay in stage B that is measured after turning off the source.

In order to obtain high-quality data during measurements some checks were carried out on the instrument to ensure it worked optimally. Moreover, while taking the readings the stacking and the standard deviation did not exceed 2 and 1 respectively. Four (4) lines of about 100 meters each were established and surveyed in the area.

The pseudo-section plots of the apparent resistivity and chargeability of the four lines were subsequently developed using Res2Dinv software.

Plate 1: Magnetic and Geo-electrical Data Acquisition

3.0 Data Processing and Interpretation

3.1 Magnetic Data Processing

Firstly, the diurnal correction was carried out to remove the variations in the earth's magnetic field caused by factors such as solar wind surge which, invariably leads to magnetic storms. The magnetic data acquisition was carried out within two days, and all through the magnetometer was set at a tuning field of 33,000nT. The data for a given day were subjected to reduction according to equation 1 below.

$$\textbf{Diurnal Correction} = \textbf{Walkmag Data} - \textbf{Base Stationmag Data} + \textbf{Datum}. \quad 1$$

Before interpretation, further imperative filtering and enhancements involving mathematical and transformational simulations are performed on the data in order to narrow the observed anomalous attributes to the rock characteristics and actual geological features. The filtering tools are regional regional-residual separation, derivative computations, and source parameter imaging, (SPI).

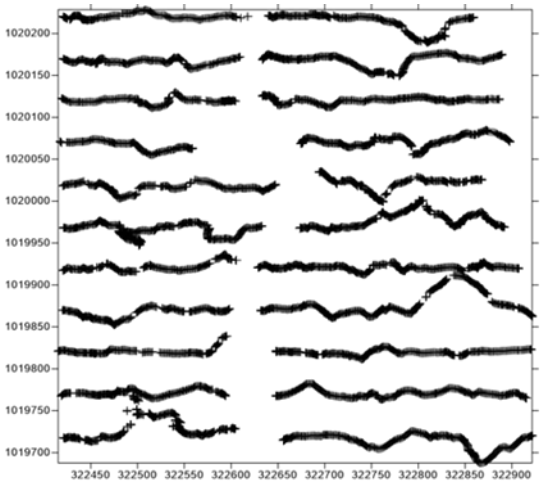

Fig. 4: TMI Data Acquisition Map

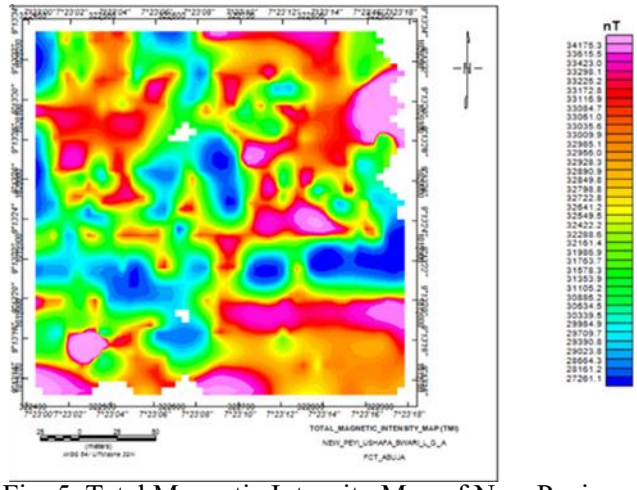

Fig. 5: Total Magnetic Intensity Map of New Peyi

The profile lines during the acquisition of Total Magnetic Intensity data are shown in Figure 4. The breaks in the lines and the bends (deviations) were due to the impassability of the fault depression that is filled with meandering streams and other natural and manmade obstructions respectively.

The total Magnetic Intensity map of New Peyi (Figure 5) was developed from the corrected magnetic data. It exposes the areas with low and high magnetic values. The magnetic field noticed at any point is the resultant of the regional and local field components as well as the remanent magnetic components of the rocks.

In the regional - residual anomaly separation, Geosoft MAGMAP software - which is based on the least square (best-fit polynomial) was deployed. Using Trend analysis, the regional field was assumed to be a first-order polynomial plane derived by the least-square fitting of a plane:

$$\boldsymbol{T(a,b) = (m_0 + m_1 a + m_2 b)} \qquad \mathbf{2}$$

where a and b are unit spacings along the two axes of the area; and $\boldsymbol{m_0}$, $\boldsymbol{m_1}$ and $\boldsymbol{m_2}$ are the coefficients of the plane. From Equation 2 above, the regional gradients were computed line by line. The result was deducted from the correlated total magnetic field intensity to obtain the residual component which is due to restricted geological features. The residual magnetic anomaly map depicts where the anomalies occupy away from the regional consequences.

While carrying out this filtering process the wavelengths and the amplitude variations of the host rocks played a major part.

In the case of vertical derivatives, Fast Fourier Transform (FFT) is put into application on gridded data to generate the filters. Foss, (2011) showed that the vertical derivative calculations are carried out by the multiplication of the amplitude spectra of a particular field by a factor of the form, $\frac{\mathbf{1}}{\mathbf{m}}\left[\left(\mathbf{u_x}^2 + \mathbf{u_y}^2\right)^{\frac{1}{2}}\right]^{\mathbf{m}}$; where m is the degree of the vertical derivative; $\mathbf{u_x}$ and $\mathbf{u_y}$ are respectively the wavenumbers in the x and y directions.

First vertical derivative filtering increases the short-wavelength portions of a field and consequently eliminate the longer-wavelengths, (i.e., the regional effects); thereby resolving the effects of adjacent anomalies, - i.e., defines the boundaries of geologic features.

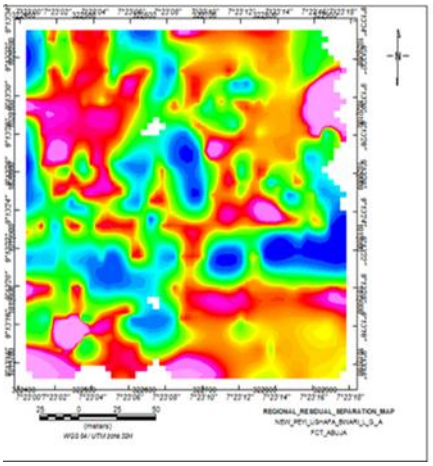

Fig. 6: Regional Residual Map of New Peyi

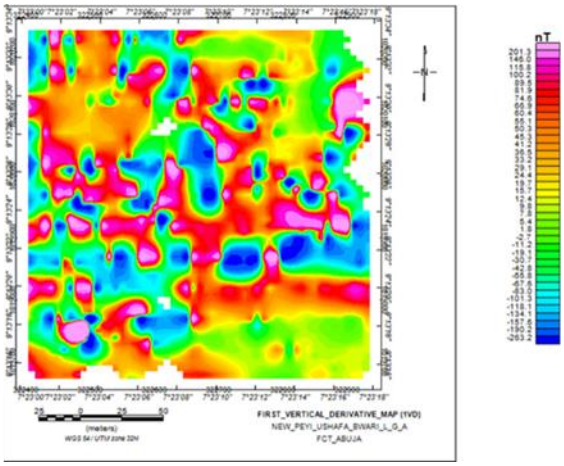

Fig. 7: First Vertical Derivative Map of New Peyi

Luo et al., (2011) showed that the analytical signal filtering accounts for both the vertical and horizontal derivatives over the entire directions of the earth's field, as well as the origin of the magnetization. Roest et al., (1992), obtained the amplitude of the analytic signal using three perpendicular gradients of the total magnetic field by applying the mathematical equation:

$$|\mathbf{AS}(\mathbf{x},\mathbf{y})| = \sqrt{\left(\frac{\partial \mathbf{T}}{\partial \mathbf{x}}\right)^2 + \left(\frac{\partial \mathbf{T}}{\partial \mathbf{y}}\right)^2 + \left(\frac{\partial \mathbf{T}}{\partial \mathbf{z}}\right)^2} \quad 3$$

$$\partial \mathbf{x} = \mathbf{grid\ interval\ in\ x-direction}$$

$$\partial \mathbf{y} = \mathbf{grid\ interval\ in\ y-direction}$$

$$\mathbf{T} = \mathbf{total\ magnetic\ field\ vector}$$

The analytic signal maximum value defines the edges and positions of a magnetic body irrespective of any remanent magnetization in the sources.

The Source Parameter Imaging (SPI) estimates the magnetic source depth from the local wavenumber of the analytical signal.

For the magnetic field T, the local wavenumber is given by:

$$\mathbf{k}(\mathbf{x},\mathbf{y}) = \frac{\frac{\partial^2 \mathbf{T}}{\partial \mathbf{x}\partial \mathbf{z}}\frac{\partial \mathbf{T}}{\partial \mathbf{z}} + \frac{\partial^2 \mathbf{T}}{\partial \mathbf{y}\partial \mathbf{z}}\frac{\partial \mathbf{T}}{\partial \mathbf{y}} + \frac{\partial^2 \mathbf{T}}{\partial \mathbf{z}^2}\frac{\partial \mathbf{T}}{\partial \mathbf{x}}}{\left(\frac{\partial \mathbf{T}}{\partial \mathbf{x}}\right)^2 + \left(\frac{\partial \mathbf{T}}{\partial \mathbf{y}}\right)^2 + \left(\frac{\partial \mathbf{T}}{\partial \mathbf{z}}\right)^2} \quad 4$$

and

$$\mathbf{k} = \frac{\mathbf{h}}{\mathbf{h}^2 + \mathbf{x}^2} \quad 5$$

Here, $\mathbf{h}$ is the depth.

At the maximum value of the local wave number k_{max}, x = 0 (i.e., located exactly above the edges of the magnetic body).

The depth (h) at this point is

$$\mathbf{h}_{(\mathbf{x}=\mathbf{0})} = \frac{\mathbf{1}}{\mathbf{k}_{\mathbf{max}}} \quad 6$$

In Oasis Montaj software this depth was established using the pre-processed residual grid as input grid data, dx, dy and dz. The output derivative was used to generate new database which was set as default, sticking to the first order derivative. Applying some computational processes - “Grid and Image”, “Minimum Curvature”, “SPI value to grid”, and then “Depth”-, the SPI map (figure 9) was generated.

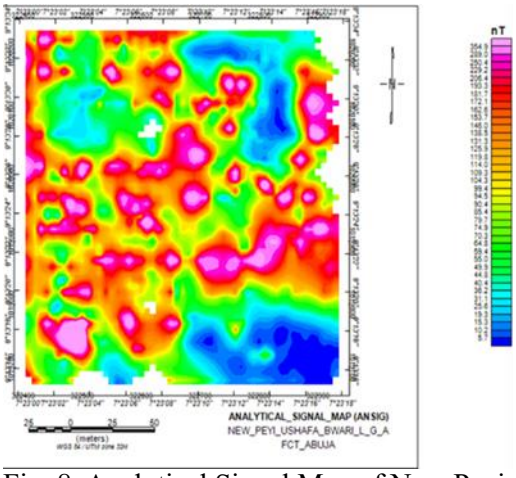

Fig. 8: Analytical Signal Map of New Peyi

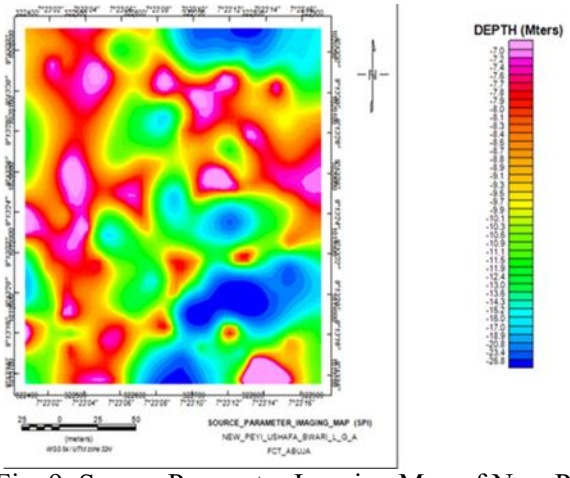

Fig. 9: Source Parameter Imaging Map of New Peyi

3.2 Interpretation of Magnetic Survey Data

The Total Magnetic Intensity Map of New Peyi (figure 5) shows zonation and alteration which are suggestive of the presence of hydrothermal alteration, usually associated with mineralization that might be due to intrusion. The TMI represents the magnetic intensity field of the New Peyi area with value ranging from 27261.1nT to 34175.3nT.

The anomaly minima and maxima amplitude variation of the residual map (figure 6) might have been caused by the presence of geological structures (faults and fractures). The residual values range from -4643.3nT to 2310.3nT, which is characterized by regions with low negative amplitudes, thereby having high wavelengths. The implication is that the causative body is not deep-seated.

The contrasting susceptibility is indicative of the suitability of the magnetic method of exploration in the area. The residual magnetic map indicated that the anomalies seem to trend N-S and NE- SW structurally. The discontinuities noticed may be likely the product of tectonic activity/magmatic intrusions.

The first vertical derivative allows for the observation of the near-surface magnetic anomaly in the area. It sharpens the anomalies over bodies, reduce anomaly complexity, thereby producing vivid image of the causative body, (figure 6).

The delineation of the boundaries of the causative body responsible for mineralization was enhanced by the analytical signal. It traces the edges of dome shaped intrusives, folded structures like synclines, anticlines and sub basins filled with metallic ores. It enhances the edges of the bodies to identify the geologic boundaries - See (figure 8).

The Source Parameter Imaging (SPI) map, (figure 9) indicated the range of depth to magnetic sources to be from 7.0 m to 26.8 m, (i.e., the depth of occurrence of mineralization is less than 27m).

3.3 Geo-electrical Data Processing

Resistivity imaging and induced polarization (IP) survey was carried out simultaneously using the ABEM SAS 1000 Terrameter, and the RES2Dinv software was used for the production of the 2-d inversion and pseudo-sections of the resistivity and Induced Polarization data. Four (4) lines of about 100 meters each were covered.

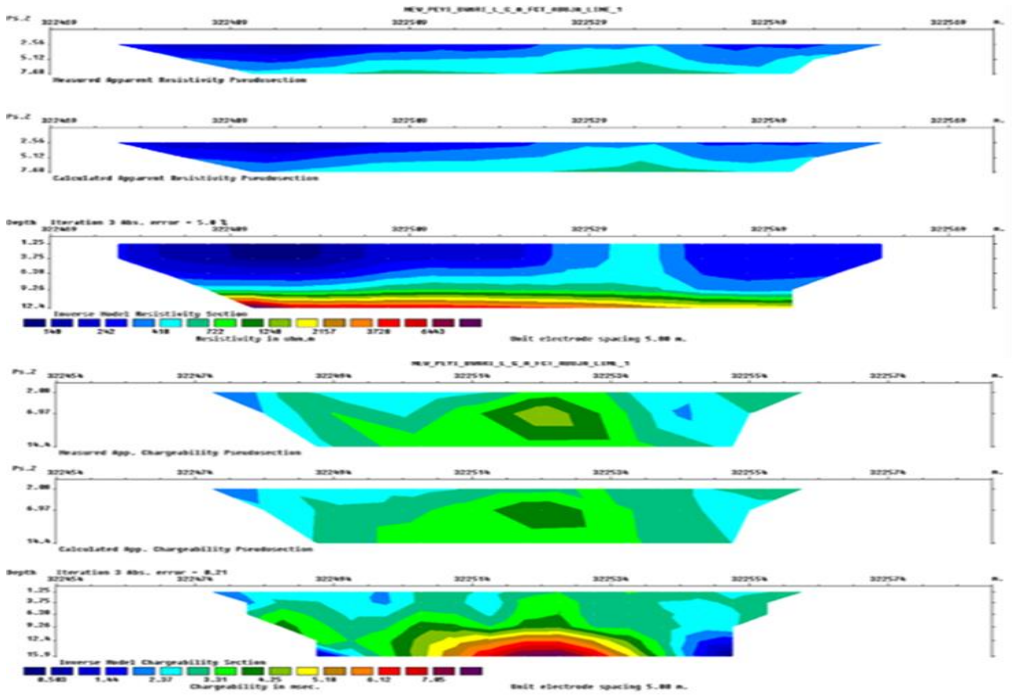

Fig.10: Line 1 Apparent Resistivity and Chargeability Pseudo-section Plots (322476.5 – 322561.5; 1019855)

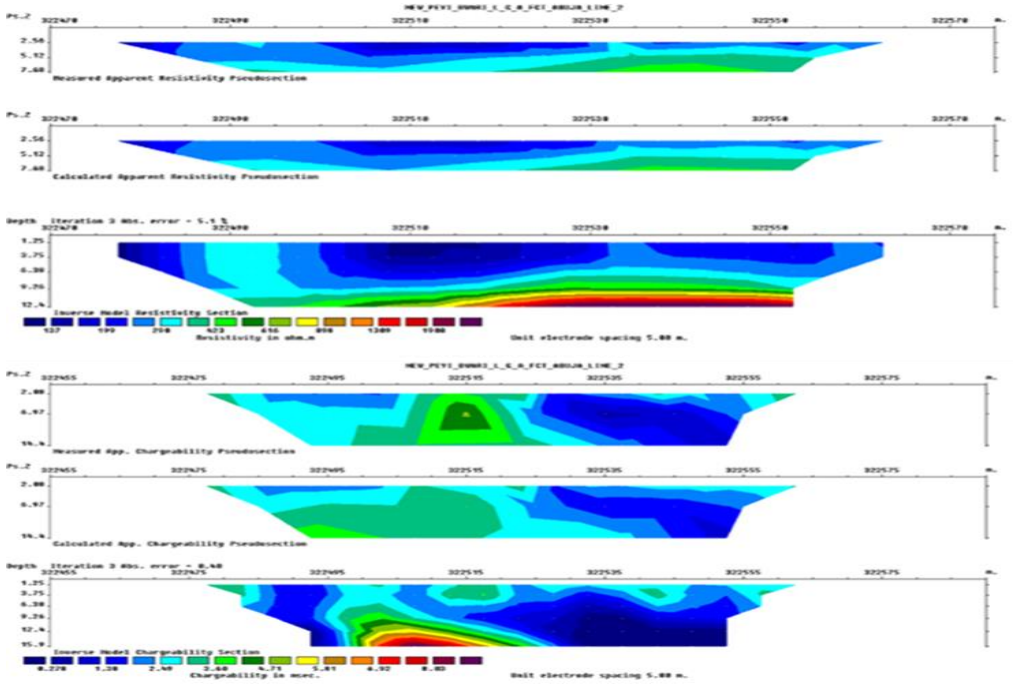

Fig.11: Line 2 Apparent Resistivity and Chargeability Pseudo-section Plots (322477.5 – 322562.5; 1020220)

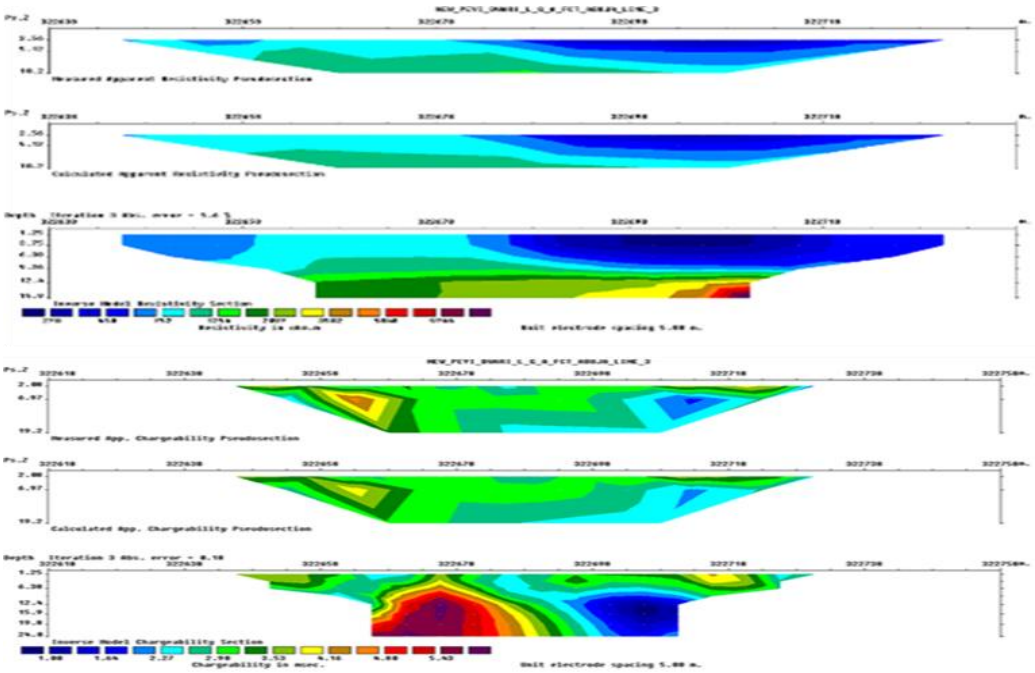

Fig. 12: Line 3 Apparent Resistivity and Chargeability Pseudo-section Plots (322730.5 – 322668.5; 102160)

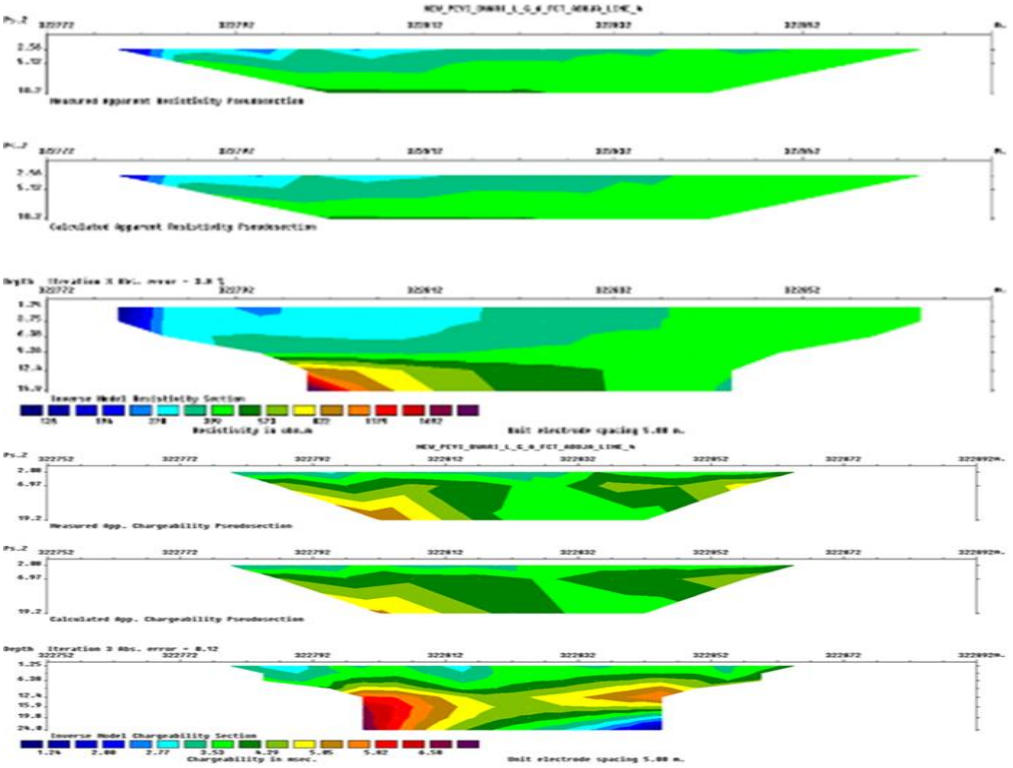

Fig. 13: Line 4 Apparent Resistivity and Chargeability Pseudo-section Plots (322864.5 – 322802.5; 101978)

3.4 Interpretation of Geo-electrical (Resistivity & Induced Polarization) Data

Figures 10 to 13 show the apparent resistivity and the chargeability pseudo section maps of the area at different lines of latitudes with varying longitudes. The observed apparent resistivity and induced polarization (chargeability) data represent an idea of the resistivity and chargeability distribution of the subsurface. Hosts with high and low resistive layers were characterized at different depths. The chargeability pseudo section maps, indicates areas with high and low chargeability and the occurrence of mineralization.

The presence of sulphide in association with gold mineralization in schist belts is responsible for the high chargeability which becomes a major factor in prospect detection and delineation. In this study the targets are high apparent resistivity (less conductive) and high chargeability for sulphide mineralization. Gold is less conductive but highly chargeable since the ore might be disseminated.

High apparent resistivity is targeted because quartz veins mostly host primary gold mineralization. Quartz/quartzites have high resistivity (low conductivity); therefore, they become an imperative factor in prospecting and delineation of gold deposits.

The design of the resistivity/IP survey could not determine the approximate length and orientation of the mineralized zones because the survey was carried out with limited number of profile lines which are far apart and unidirectionally oriented.

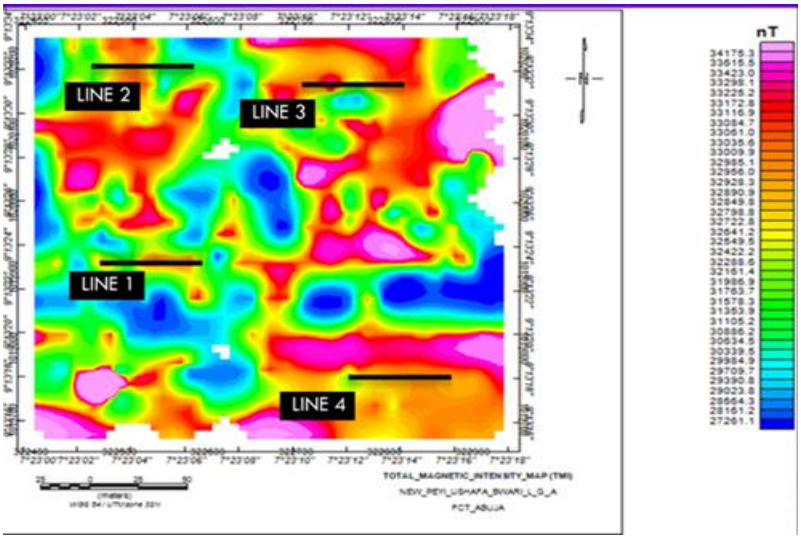

Fig. 14: Positions of the Geo-electric Survey Lines in Relation to the Total Magnetic Intensity Map

4.0 Results of Field Study

This study utilized ground magnetic and geoelectrical (resistivity/induced polarization) methods as survey tools for the search for suspected gold mineralization. During the magnetic survey, an inter profile spacing of 50 meters was used to give more detailed coverage using GSMP – 25 Potassium Magnetometer.

The geo-electrical profiling was designed utilizing Wenner method, using chargeability equipment (Terrameter SAS 1000) to determine the nature and mode of occurrence of the gold deposits. The study

established the orientation of the structures to be N-S and NE-SW, being the dominant fracture directions, which control the boundaries of the mineralization.

Presently there are widespread excavations within and around the project area due to the illegal activities of artisanal miners which have caused widespread environmental degradation, geotechnical alterations of the ground, health hazards, and death. The results of this research work, having delineated potential areas with gold mineralization, would consequently, lead to target mining. This would invariably lead to the reduction of widespread environmental degradation and the averting of the other challenges enumerated above.

5.0 Conclusions

The applied geophysical methods (magnetics, electrical resistivity and the induced polarization) was able to define the structural, magnetic anomaly and the electrical anomaly patterns in the study area. The mineralization finds potential hosts in these structures which corresponds with the edges of the magnetic bodies detected. The depth to magnetic source was established using ground magnetic method.

Furthermore, some structures in this area could be mineralized quartz veins. The responses to physical parameters from the magnetic data also revealed the presence of both conductive and non-conductive structures. Most of them are within resistive hosts and while the others are located within conductive hosts. The dominant structural orientation is mostly N-S and NE-SW as established.

Acknowledgements

My special and stupendous gratitude to the Almighty God is quite candid for the grace I received in achieving this feat.

I am deeply indebted to my chief supervisor and supervisor, Dr. Martin Ogharandukun and Mr. Patrick Dikedi respectively, for their tireless and painstaking supervision and evaluation throughout the period of this project work, not minding their tight schedules. My External Examiner, Professor Abu Mallam is deeply appreciated as well.

Furthermore, I sincerely thank and appreciate the indefatigable Head, Department of Pure and Applied Physics, Dr. Ofe Uko, for his time and meticulosity in correcting some technical and grammatical errors throughout the period of compiling this project work. I wish to also extend my gratitude to the Deans, Faculty of Natural and Applied Sciences and School of Post-Graduate Studies, Professors Simon Okwute and Gabriel Egbe for their good leadership and friendliness.

Of course, I could not have feigned ignorance of the contributions and moral support I got from all my lecturers, entire members of staff of the Department of Pure and Applied Physics, as well as those in the School of Post-Graduate Studies of this amiable institution, Veritas University, Abuja. May the good Lord Jesus Christ bless and preserve you.

Worthy of mention are my two professional colleagues; Okolo, Ikechukwu Thaddeaus and Akinde, Aderibigbe S. who sacrificed their time, energy, talent and resources in the course of the data acquisition and processing.

My sincere thanks also go to members of my family – my mother, siblings, wife, children and all others whom space and time could not allow me to mention here. I am sincerely grateful to all.

Open Research

Data Availability Statement

Data: All the data presented in this paper were acquired from the field. The raw and corrected magnetic data as well as the geoelectric data (resistivity and induced polarization) used in this paper are available at http://github.com/Stephen-Udeh/Stephen-Udeh.

The walkmag data link could be found in Stephen-Udeh/WALK_MAG_DATA.txt at main · Stephen-Udeh/Stephen-Udeh (github.com).

The stacked data link is Stephen-Udeh/STACKED_MAG_DATA.csv at main · Stephen-Udeh/Stephen-Udeh (github.com).

Data links for base station Stephen-Udeh/BASE_MAG_DATA.txt at main · Stephen-Udeh/Stephen-Udeh (github.com) and Stephen-Udeh/CORRECTED_DATA.txt at main · Stephen-Udeh/Stephen-Udeh (github.com).

The links for the geoelectric data are:

Line 1: Stephen-Udeh/NEW_PEYI_LINE_1_RESIS.DAT at main · Stephen-Udeh/Stephen-Udeh (github.com)

Stephen-Udeh/NEW_PEYI_LINE_1.DAT at main · Stephen-Udeh/Stephen-Udeh (github.com)

Line 2: Stephen-Udeh/NEW_PEYI_LINE_2_RESIS.DAT at main · Stephen-Udeh/Stephen-Udeh (github.com)

Stephen-Udeh/NEW_PEYI_LINE_2.DAT at main · Stephen-Udeh/Stephen-Udeh (github.com)

Line 3: Stephen-Udeh/NEW_PEYI_LINE_3_RESIS.DAT at main · Stephen-Udeh/Stephen-Udeh (github.com)

Stephen-Udeh/NEW_PEYI_LINE_3.DAT at main · Stephen-Udeh/Stephen-Udeh (github.com)

Line 4: Stephen-Udeh/NEW_PEYI_LINE_4_RESIS.DAT at main · Stephen-Udeh/Stephen-Udeh (github.com)

Stephen-Udeh/NEW_PEYI_LINE_4.DAT at main · Stephen-Udeh/Stephen-Udeh (github.com)

References

Alabi A. A., Abdullahi S. (2018): Geophysical Evaluation of Gold Potential in Southeastern Part of Kafin-Koro, Northwestern Nigeria. *Journal of Geosciences and Geomatics*.; 6(3):153-164. Doi: 10.12691/jgg-6-3-6. http://www.sciepub.com/journal/JGG

Chuku, D. U. (1981): Distribution of gold mineralization in the Nigeria basement complex in relation to orogenic cycle and structural setting, in the Precambrian geology of Nigeria. A publication of the Geological Survey of Nigeria, 177-194.

Foss, C. (2011): Magnetic data enhancement and depth estimation. In H.K Gupta. encyclopedia of solid earth geophysics. Springer Science + Business Media B.V. Magnetic_Data_Enhancements_and_Depth_Est Fo C..pdf

Luo, Y., Wang, M., Luo, F., and Tian, S. (2011): Direct analytical signal interpretation of potential field data using 2-D Hilbert transform. Chinese Journal of Geophysics Vol. 54, 551-559. LUO_et_al-2011-Chinese_Journal_of_Geophysics.pdf

Mbonimpa, A.B., Barifaijo, E. and Tiberindwa, J.V. (2007): The potential for gold mineralization in the greenschist belt of Busia District, South Eastern Uganda. African Journal of science and technology, 8 (1), 116-134. ajol-file-journals_83_articles_155944_submission_proof_155944-985-407042-1-10-20170512 (1).pdf

NGSA, (2004): Modified geological map of Abuja from Nigerian Geological Survey Agency. Geological map of Abuja showing the rock types and sampling points... | Download Scientific Diagram (researchgate.net)

Obaje, N. G. (2009): Geology and mineral resources of Nigeria. In P. N. Obaje, lecture notes in earth sciences (p. 14). Keffi, Nasarawa: Springer Dordrecht Heidelberg London New York. Geology and Mineral Resources of Nigeria - Nuhu George Obaje - Google Books

Roest, W.R., Verhoef, J., and Pilkington, M., (1992): Magnetic interpretation using the 3-D analytic signal. Geophysics, 57,116-125. Roest1992GEO.pdf

Udeh, Stephen, (2023): http://github.com/Stephen-Udeh/Stephen-Udeh. [Collection]